THE JOURNAL OF PHYSICAL CHEMISTRY C
A JOURNAL OF THE AMERICAN CHEMICAL SOCIETY

pubs.acs.org/JPCC

Article

Light-Induced EPR Study of Polymorphic Acene-Stipulated Transition in P3DDT:$PC_{61}BM$ Composite

Victor I. Krinichnyi,* Evgeniya I. Yudanova, and Nikolay N. Denisov

Cite This: *J. Phys. Chem. C* 2022, 126, 4495−4507

Read Online

ACCESS | Metrics & More | Article Recommendations

ABSTRACT: We report the light-induced electron paramagnetic resonance (LEPR) and optics study of spin charge carriers initiated by light photons with the energy of 1.34−4.52 eV in the initial and slightly acene-treated composites of a regioregular poly(3-dodecylthiophene) (P3DDT) with a [6,6]-phenyl-C_{61}-butyric acid methyl ester ($PC_{61}BM$). Light irradiation leads to the formation in both polymorphs of spin charge carriers, polarons, and methanofullerene radical anions. Magnetic resonance, relaxation, and dynamic parameters of such carriers depend on the energy of exciting light photons as well as on a balance of a chaotically structured polymer α-polymorph with spin traps and a more structured its β-polymorph. The charge carriers, photoinitiated in the α-polymorph, are characterized by an extreme dependence of their main parameters from the energy of exciting photons. The increase in the concentration and stability of both mobile charge carriers were reached upon modification of the initial composite by the simplest conjugated acenes. The greatest effect was registered for the composite, weakly doped by naphthalene molecules. The concentration and other properties of charge carriers photoinitiated in a modified composite were found to correlate with the band structure of the acene introduced. Such an effect was interpreted in favor of a triggerlike polymorphic $\alpha-\beta$ transition stipulated in the system by planar acene molecules. It leads to an acceleration of spin−lattice relaxation of mobile charge carriers, a decrease in the anisotropic diffusion of polarons between polymer chains, and a slow down of the recombination of charge carriers. This opens horizons to use optimally acene-doped polymers and their composites for the creation of electronic and spintronic devices with spin-photon-assisted parameters.

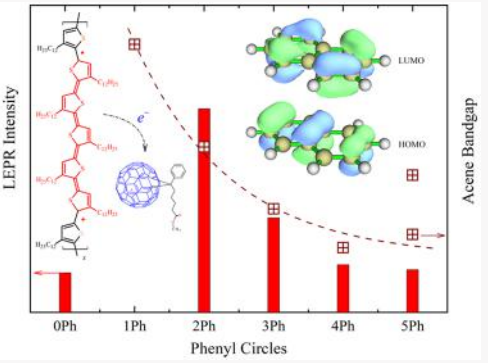

1. INTRODUCTION

Organic donor−acceptor composites are considered promising materials for creating various molecular devices, such as field-effect transistors, switches, sensors, and photovoltaic elements.[1−3] The latter normally consist of a polymer matrix with embedded allotropes of carbon (fullerenes, graphene, and carbon nanotubes) and other small molecules. Light irradiation initiates a formation in such bulk heterojunctions (BHJ) of excitons, which may dissociate into positively charged polarons on polymer chains and negatively charged fullerene or nonfullerene radical anions situated between the polymer chains. The functionality and effectiveness of such devices significantly depend on the structure of their ingredients used, as well as on solvent, temperature, molecular weight, sample preparation, and possible treatments. These factors play a key role in BHJ structuring, so the structure−property correlations of organic semiconductors are mainly studied via chemical modifications such as regioregularity control and side-chain engineering.[4] Currently, there is a strong effort toward understanding and controlling the relation between BHJ morphology and electronic properties of molecular devices with polymer and copolymer matrices. For example, polymorphism has been found for the copolymer composed of naphthalene diimide and bithiophene units[5] which after dissolving in a nonsuitable solvent showed an extra absorption optics peak at lower photon energies, indicating the formation of a secondary aggregated phase. Two distinctly semicrystalline polymorphs with different optical band gaps, photoluminescences, π-stacking distances, hole mobilities, and photogeneration efficiencies were identified in a low-band-gap diketopyrrolopyrrole polymer.[6] Poly(3-alkylthiophenes) (P3AT), poly(3-hexylthiophene) (P3HT),[7−9] poly(3-dodecylthiophene) (P3DDT),[10,11] and other conjugated polymers[12−14] also exhibit polymorphism because they consist of an amorphous "spaghetti-like" phase (α-polymorph) and an aggregated phase (β-polymorph) with relatively ordered crystalline regions.[15] Two differently ordered H-type aggregates were identified in P3HT at extremely low temperature by Franck−Condon analyses of its

Received: December 8, 2021
Revised: February 12, 2022
Published: March 1, 2022

https://doi.org/10.1021/acs.jpcc.1c10407
J. Phys. Chem. C 2022, 126, 4495−4507

emission spectra.[9] An end-to-end packing of P3DDT lamellae was shown[11] to predominate in its first polymorph, whereas the second one has interdigitated side chains with reduced lamellar spacing. Such morphology causes the band dispersions in the direction perpendicular to the layer. This bandwidth broadening, in turn, decreases the energy band gap.[16] The balance of these polymorphs formed in P3AT is governed by polymer structure and conditions of synthesis and can be controlled by their molecular weight,[17] the evaporation rate of solvent,[18] exposure to solvent vapors,[19] and thermal annealing.[20] When the polymer crystallinity increases, its morphology becomes more planned, its chains form two-dimensional (2D) stacks. Interlayer spacing of the coplanar P3AT chains increases with the side chain length because the alkyl side chains act as spacers between them.

Because the changes in optical and electronic properties of polymer devices depend on the structural differences between the polymorphs, that allows controlling of polymer self-organization for developing next-generation electronic devices. This is especially important for photovoltaic devices with a polymer matrix and spin charge carriers. The efficiency and functionality of such systems are determined by their structure and morphology that govern spin-assisted separation, coupling, and recombination of charge carriers formed after dissociation of initial excitons. Improving these properties can be achieved upon modification of polymer:fullerene BHJ with various small carbon allotropes (nanotubes, graphene)[21] or 2D hydrocarbons.[22] Zhang et al. showed[14] that adding three percent of di-iodooctane molecules into PTB7:$PC_{71}BM$ BHJ leads to a 2-fold increase in its power conversion efficiency (PCE) due to a decrease in the number of charge carrier traps and also reduction of bimolecular recombination rate. This parameter of the P3HT:$PC_{61}BM$ composite increases by 13% upon addition of the same quantity of galvinoxyl molecules.[7] Such an effect was explained by resonant exchange interaction of spin adducts with acceptors accompanied by their singlet−triplet conversion without changing the morphology of the sample. A more significant PCE increase was obtained when adding a small quantity of butyl 1-pyrenebutirate into fullerene-modified P3HT films.[23] This enhancement was explained in favor of limiting the aggregation of fullerene molecules and improving the morphology of the active layer due to such a procedure. The operation stability of photovoltaic devices can also be enhanced by increasing the exchange interaction between the host and guest small molecules.[24] This is evident that the comprehensive studies of polymorphism of crystalline phases in conjugated polymers are limited and their results are patchy and ambiguous. The relation between their structure and properties of charge carriers is still not clear, so then the influence of molecular additives on the system's structural and morphological properties remains the subject of discussion.

In the study of the initial and modified BHJ are commonly used optical, voltammetric, calorimetric, and other experimental methods. However, light-induced electronic paramagnetic resonance (LEPR) spectroscopy became one of the most used methods for the study of such systems. This is mainly due to two circumstances. The first of them is the stabilization or/and photoinitiation in donor−acceptor BHJ of charge carriers possessing unpaired electrons, and the second reason is the fact that the domestic carriers take part in all processes carried out in these compounds. Thus, this method allows us to register separately these paramagnetic centers, determine their magnetic resonance, relaxation, and dynamic parameters for getting structure-electronic correlations of conjugated polymers and their composites.[25,26] For example, Carati et al.[13] showed by the LEPR method that slight doping of the PTB7:C_{60} BHJ with butyl 1-pyrenebutirate leads to a sufficient (2- to 4-fold) change of spin−lattice relaxation of fullerene radical anions due to fullerene−pyrene interaction. It was concluded that such interaction prevents recombination of charge carriers, however, without noticeable change of BHJ morphology. However, an additional introduction of optimal amount (3−6 wt %) of 1,2-benzopyrone or 2,5-diphenyloxazole molecules into the P3DDT:$PC_{61}BM$ BHJ,[27] and the latter additive into the copolymer composite PBDB-T:$PC_{61}BM$[28] was shown to increase/decrease the number of mobile/localized charge carriers, increase their stability and exchange $\pi-\pi$-interaction. It was suggested that such an improvement in the electronic properties of the fullerene-based composite could occur due to partial ordering of the sample matrix upon its doping, as it occurs in nonfullerene photovoltaic system.[24] The concentration, composition, and dynamics of spin charge carriers was found to be governed not only by the BHJ modification with small molecules but also by the number, spatial distribution, and energetic depth of spin traps formed in the disordered polymer matrix as well as the energy of the light exciting photons.

Thus, the molecular ordering of various polymer systems is characterized by the crystalline, dynamic, and static nematic parameters of differently packed phases. These parameters are linked to molecular and electronic dynamics, distributions of coupling spin charge carriers, and their traps formed in a disordered matrix. The LEPR spectroscopy seems to be an ideal instrument for the study of polymorphic spin-assisted $\alpha-\beta$-transitions in such organic semiconductors controlled by their chemical modification or/and physical impacts.

Hereby, we report the results of a detailed comparative continuous wave (cw) LEPR study of spin-dependent excitation, relaxation, dynamics, and recombination of charge carriers photoinitiated in the initial and slightly doped with several simplest acenes P3DDT:$PC_{61}BM$ BHJ. Among P3AT, regioregular P3DDT is characterized by mostly extended side alkyl substituents. They act as insulating envelopes of its π-conjugated chains and, therefore, should to prevent more effectively an interaction of intrinsic charge carriers with their spin environment. Isotropic Landé splitting factors of polarons, g_{iso}^{P}, and C_{60}-based methanofullerene, g_{iso}^{mF}, differ significantly, so the EPR spectra are separately registered and well-customized. This was the reason that they were chosen as previously,[27] as electron-donating and charge-accepting moieties, respectively. Acenes are characterized by the most conjugate and planar structure. Therefore, the use of these small molecules as additives could be expected to more increase intermolecular $\pi-\pi$-interaction in the P3DDT:$PC_{61}BM$ composite, improving its ordering and energy-conversion properties. The data obtained allowed us to find the correlations interconnecting the main spectral resonant parameters of spin charge carriers with the structure, composition of the samples studied, as well as with energy of the initiating light photons. This should more greatly clarify the key role of the conjugation degree of small molecules in structuring the initial polymer composite, which improves its energy-converting functionality due to the higher stability of spin charge carriers.

2. EXPERIMENTAL SECTION

2.1. Materials Used in Experiments. In this work, regioregular poly(3-dodecylthiophene) (P3DDT) with the

https://doi.org/10.1021/acs.jpcc.1c10407
J. Phys. Chem. C 2022, 126, 4495−4507

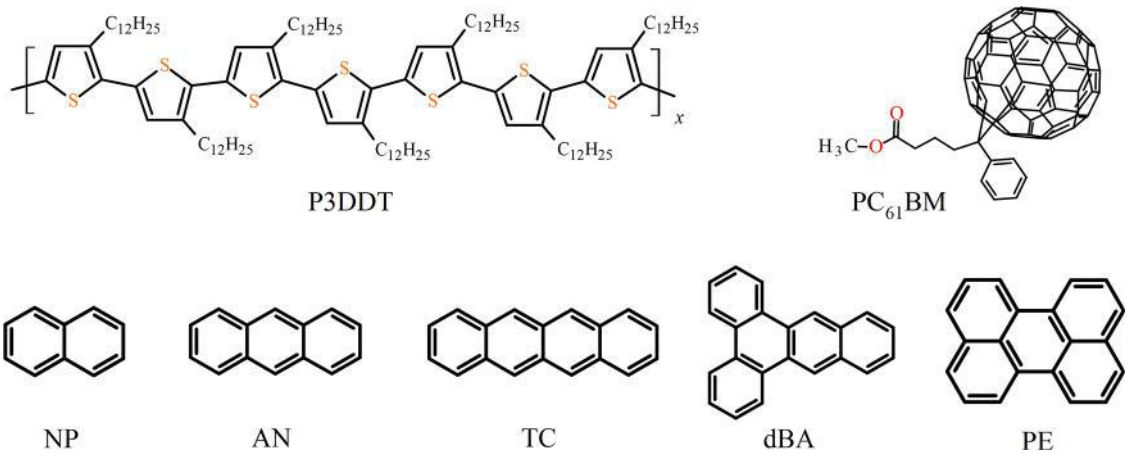

Figure 1. Schematic structures of the regioregular poly(3-dodecylthiophene) (P3DDT), [6,6]-phenyl-C_{61}-butanoic acid methyl ester ($PC_{61}BM$), naphthalene (NP), anthracene (AN), tetracene (TC), dibenz[a,c]anthracene (dBA), and perylene (PE) used for the preparation of polymer composites.

lattice constants of a = 2.583 nm, b = 0.775 nm, and c = 0.777 nm,[29] distributed by Aldrich (USA), and [6,6]-phenyl-C_{61}-butanoic acid methyl ester ($PC_{61}BM$) distributed by Solenne BV (The Netherlands) were used without additional purification as electron-donating and accepting groups, respectively. Their band gap or difference of the lowest unoccupied molecular orbital (LOMO) and highest occupied molecular orbital (HOMO), $\Delta E_g = E_{LUMO} - E_{HOMO}$, was determined experimentally to be 1.74 eV[30] and 2.35 eV,[31] respectively. For the doping of the P3DDT:$PC_{61}BM$ composite up to y = 0.06 level were used naphthalene (NP), anthracene (AN), tetracene (TC), dibenz[a,c]antracene (dBA), and perylene (PE). The chemical structures of all ingredients are shown schematically in Figure 1.

2.2. Preparation of the Composites. An initial P3DDT:$PC_{61}BM$ composite was prepared according to the procedure reported elsewhere.[27] First, the polymer and methanofullerene were dissolved in dichlorobenzene to achieve a concentration of 5.5 mg/mL. Then the resulting solution was heated at T = 333 K for 10 min until the ingredients were completely dissolved. Additives were dissolved separately in dichlorobenzene until their weight concentration reaches 6 mg/mL. The first solution was mixed with the additive ones in a quantity enough to reach a polymer/methanofullerene/corresponding additive weight concentrations ratio of 1:1:0.06. The resulting solutions were treated in ultrasonic cleaner DADI DA-968 (P = 50 W) for 10 min, followed by heating for 10 min at T = 333 K and secondary ultrasonic treatment within 10 min. Finally, they were cast 7 times (5 μL) into both sites of a separate ceramic plate with subsequent drying in air until the formation of films with the size of ca. 4 × 8 mm^2 and thickness of ca. 0.1 mm on both sides of the plate. As a result of this procedure, the initial donor−acceptor P3DDT:$PC_{61}BM$ composite and this sample doped with the scenes up to the level of y = 0.06 were obtained. The molecular ratio, that is the numbers of DDT monomers, as well as methanofullerene and dopant molecules, of the P3DDT:$PC_{61}BM/NP_{0.06}$ sample was determined to be 4.97:1.37:1.00. This ratio for the P3DDT:$PC_{61}BM/AN_{0.06}$ sample was determined to be 6.87:1.89:1.00.

2.3. NIR−Vis−UV Absorption Spectra of the Initial and Acene-Modified Polymer Composites. Optical absorption spectra of the initial P3DDT:$PC_{61}BM$ and slightly doped composites were obtained at T = 298 K by using a spectrophotometer (Specord-250-plus, Analytik Jena) scanning within the band 1.13−6.20/1100−200 eV/nm. The spectra are shown in Figure 2. They consist of the spectral components whose positions were determined accurately by using the differentiation procedure.

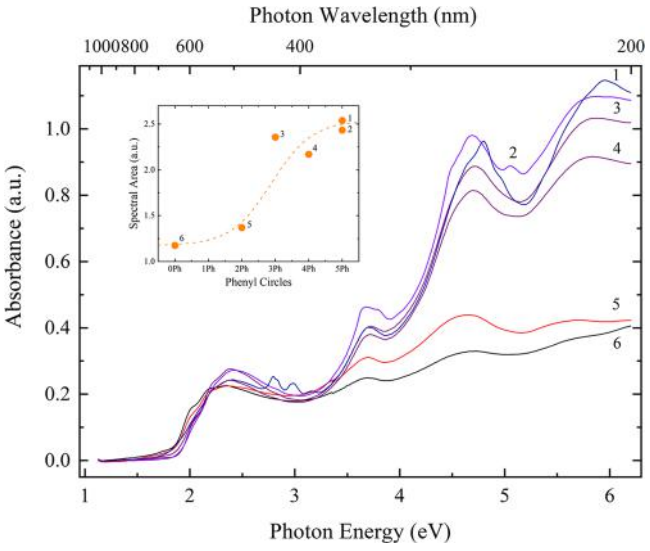

Figure 2. NIR−vis−UV absorption spectra of the P3DDT:$PC_{61}BM/PE_{0.06}$ (1), P3DDT:$PC_{61}BM/dBA_{0.06}$ (2), P3DDT:$PC_{61}BM/AN_{0.06}$ (3), P3DDT:$PC_{61}BM/TC_{0.06}$ (4), P3DDT:$PC_{61}BM/NP_{0.06}$ (5), and P3DDT:$PC_{61}BM$ (6) samples obtained at T = 298 K. In the inset is shown an effective concentration of photons absorbed by the initial and acene-doped composite P3DDT:$PC_{61}BM$ as a function of the phenyl circles of additive. The dashed line is drawn arbitrarily only for illustration to guide the eye.

2.4. Photoexcitation of Spin Charge Carriers in the Samples. The samples situated in the center of the MW cavity of the EPR spectrometer were illuminated through cylindrical quartz light guide by an achromatic, white light source with the correlated color temperature (CCT) of T_c = 5000 K and monochromatic sources with the photon energy/wavelength of 1.34−4.52 eV/923−275 nm and spectrum half-width of 12−15 meV/10−12 nm based on high-power (5−10 W) 3535SMD

https://doi.org/10.1021/acs.jpcc.1c10407
J. Phys. Chem. C 2022, 126, 4495−4507

light-emitting diodes (LEDs) distributed by the Sumit-Lighting Co., Ltd. Optical spectra of these light sources were obtained at T = 298 K by the "Optofiber" FSD-9 spectrometer equipped with a 16-bit analog-to-digital converter as it was reported elsewhere.[28] The radiating power of the sources was determined using the IMO-2N broadband optics emission power meter in combination with LX-1010BS digital lux meter. Spectral and radiating parameters of the LEDs used in experiments are presented in Table 1. Normalizing coefficients of illumination power emitted by these sources were obtained from a comparison of their integrated optical spectra and used for further estimation of spin concentration in the composites under study.

Table 1. Wavelength (l_{ph}), Energy ($h\nu_{ph}$), Illuminance (I_{rad}), and Irradiation Power (P_{rad}) of the Achromatic[a] and Chromatic LED Sources Used for Steady-State Initiation of Spin Charge Carriers in the Composites under Study

no.	λ_{ph}, nm	$h\nu_{ph}$, eV	I_{rad}, lux	P_{rad}, mW
1	W5K	W5K	105300	235
2	922	1.34	229600	140
3	843	1.47	385400	150
4	734	1.69	188600	115
5	655	1.89	111520	68
6	627	1.98	101620	62
7	612	2.03	121360	74
8	595	2.08	49200	30
9	549	2.26	35260	21.5
10	518	2.39	82000	50
11	495	2.51	91840	56
12	488	2.54	90200	55
13	444	2.79	252260	154
14	423	2.93	152520	93
15	396	3.14	141040	86
16	381	3.25	205000	125
17	364	3.41	96760	59
18	308	4.02	246	0.15
19	275	4.52	1640	1.0

[a]Achromatic: white with the color temperature of T_c = 5000 K (W5K).

2.5. LEPR Spectra Registration and Processing. The study of the initial and modified composites was carried out using the X-band (9.7 GHz) PS100X spectrometer EPR with 100 kHz synchronous signal detection equipped with a homemade LED-based light source. MW generator provides the maximum field power of 150 mW, corresponding to its magnetic term B_1 of 48 μT in the center of MW cavity where a sample within a quartz Dewar filled with liquid nitrogen is placed. The ratio of signal-to-noise of LEPR spectra was increased by multiple field scanning. The processing and simulation of the spectra were made using the EasySpin[32] and OriginLab software. Spectral consistency and individual spin concentration were determined by deconvolution of effective LEPR spectra registered far from their MW saturation combined with the "light on−light off" procedure described elsewhere.[26,33,34] The Landé splitting g-factors of all paramagnetic centers were determined using lateral single-crystalline N,N-diphenyl-N'-picrylhydrazyl standard with an effective g = 2.0036 ± 0.0002.[35] The accuracy of estimation of the intensity I, line width, or the distance between their positive and negative spectral peaks ΔB_{pp}, and the position on the field was determined to not exceed 1.1%, ± 3.2 × 10^{-4} and ±2.5 × 10^{-4} mT, respectively. Spin relaxation times were obtained with the error varying within the interval 7−14%.

2.6. Calculation of Band Parameters of Ingredients used in Experiments. The energies E_{LUMO}, E_{HOMO}, and E_g = E_{LUMO} − E_{HOMO} of the acenes used in experiments were obtained by using the Orca program[36] with the RHF SP functional and def2-SVP basis set as well as visualization of their orbital configurations was made using the MultiWFN software.[37] These parameters are summarized in Table 2 where they are compared with those obtained by Mekenyan et al.[38]

Table 2. HOMO, LUMO, and Band Gap E_g Energies Calculated for Polycyclic Aromatic Hydrocarbons Used in Experiments[a]

acene	HOMO	LUMO	E_g	E_g^*
benzene (BE)	−9.23	3.70	12.93	7.96
naphthalene (NP)	−7.83	2.29	10.13	10.06
anthracene (AN)	−7.01	1.43	8.43	7.28
tetracene (TC)	−6.49	0.88	7.37	6.52
perylene (PE)	−6.67	1.07	7.73	6.71
dibenzanthracene (dBA)	−7.53	1.82	9.35	7.09

[a]All values are given in eV. The E_g values calculated in the present work using the Orca program with the RHF SP functional and def2-SVP basis set. The E_g^* values were obtained by Mekenyan et al.[38]

3. RESULTS AND DISCUSSION

3.1. IR−Vis−UV Spectra of the Initial and Acene-Doped Composites. Optical spectra of all the samples used in experiments are presented in Figure 2. They consist of superposed spectral contributions of the polymer P3DDT, conjugated polyaromatic additive, and fullerene derivative $PC_{61}BM$. The lines of the latter are registered at both the spectral ultraviolet and visible regions of the entire optical range used (Figure 2). They contain high-energy lines at ca. 5.84/212, 4.70/264, and 3.71/334 eV/nm,[39,40] characteristic for fullerene, as well as an extended weak band 2.88−1.82/430−680 eV/nm with a weakly pronounced superfine structure caused by the forbidden transitions in such system.[41] P3DDT adds to the spectral band the respective line at 2.38/522 eV/nm, corresponding to interband HOMO−LUMO $\pi-\pi^*$ transition between thiophene units.[42] The presence of polyacenes, as well as aromatic dopants with the branched structure, is manifested mainly as increase in the high-energy spectral region of the acene-modified composites (see Figure 2). Such an effect depends not only on structure of the polycyclic aromatic additives but also on the length of their π-conjugacy. Indeed, the data presented in the inset of Figure 2 clearly indicate a growth of the number of photons absorbed by the acene-modified samples with an increase in the aromatic cycle multiple, N_{ph}. The absorption bands of the spectra of aromatic molecules used in the study lie in the UV range, which corresponds to $\pi-\pi^*$ transition in π-conjugated systems.[43] In general, their contribution is manifested as a significant increase in the optical density of wide fullerene UV-bands with some features. Thus, the transition $^1A_1^- \rightarrow {}^1B_2^+$ adds to an effective spectrum 2 of dBA-modified sample the corresponding contributions lying around 3.80/326 eV/nm,[44] while in curve 1 obtained for PE-doped composite, narrow lines are visible when 4.68/265, 2.98/416,

https://doi.org/10.1021/acs.jpcc.1c10407
J. Phys. Chem. C 2022, 126, 4495−4507

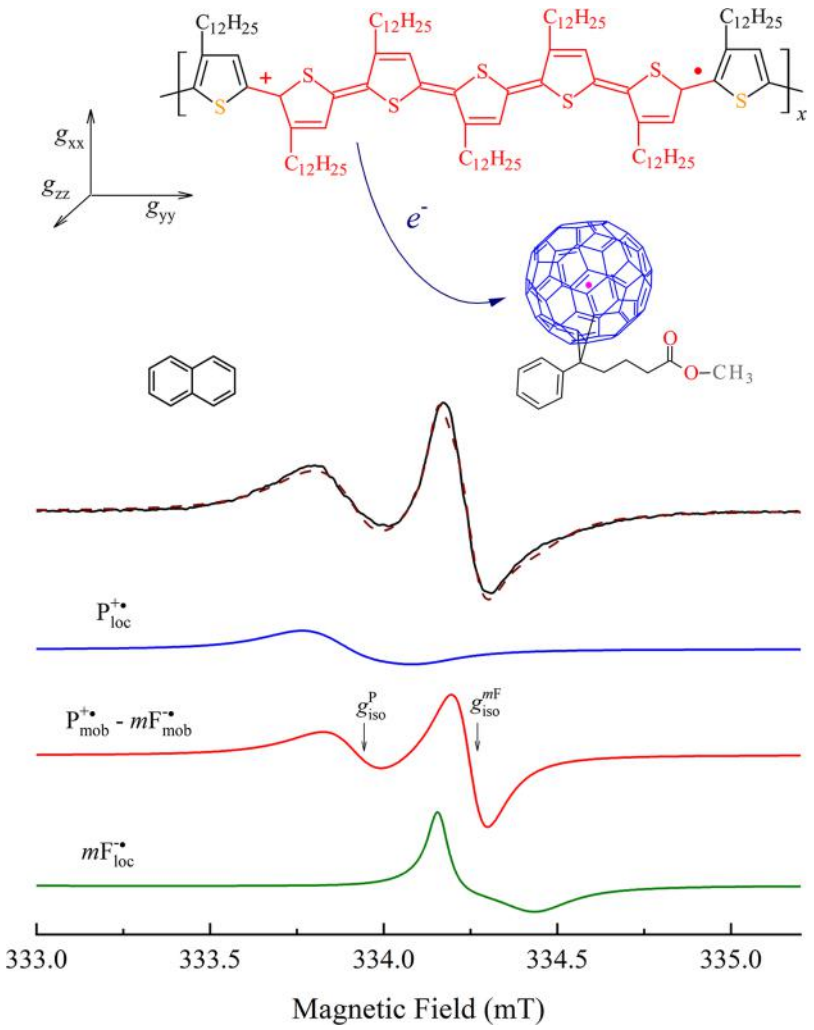

Figure 3. Effective LEPR spectra of the composite P3DDT:$PC_{61}BM/NP_{0.06}$ irradiated by white light with T_c = 5000 K at T = 77 K. Sum spectrum and its terms due to localized polarons, $P^{+\bullet}_{loc}$, radical pairs, $P^{+\bullet}_{mob} \leftrightarrow mF^{-\bullet}_{mob}$, and immobilized methanofullerene, $mF^{-\bullet}_{loc}$, calculated with relative concentrations 1.00:1.72:1.05, respectively, and the parameters presented in Table 2, are also shown.

and 2.79/444 eV/nm, corresponding to electron-oscillating transitions $^1A_1^- \rightarrow {}^1B_2^{+1}A_1^-$.[45]

3.2. Magnetic Resonance Parameters of Spin Charge Carriers Photoinitiated in the Samples. Figure 3 depicts typical different light-minus-dark LEPR spectrum of the P3DDT:$PC_{61}BM$ composite steady-state irradiated by a white light with color temperature of T_c = 5000 K at T = 77 K. As in the case of other composites of conjugated polymers and C_{60}-based methanofullerene,[26,33,46] the lines registered in low and high magnetic fields were attributed to the appearance in the sample of positively charged polarons $P^{+\bullet}$ and negatively charged methanofullerene $mF^{-\bullet}$ background photoinduced in its bulk heterojunctions, respectively. They first fill the spin traps formed in the polymer matrix due to its disordering. Being immobilized, they should demonstrate weakly anisotropic magnetic resonant parameters, such as splitting Landé g-factors, g^{P}_{ii} and g^{mF}_{ii}, and line widths that are the distance between spectral positive and negative peaks, ΔB^{P}_{pp} and ΔB^{mF}_{pp}, and are characterized by respective concentrations, n^P and n^{mF}. The subsequently formed mobile carriers should demonstrate isotropic Lorentzian contributions to the total LEPR spectrum. To determine and control these parameters of all paramagnetic centers excited in the composite understudy at the wide range of the and photon energy, effective LEPR spectra obtained with and without illumination ("light on−light off" method) should be first deconvoluted as it was described previously[26,33,46] by using parametric splitting of each spectral components $\Delta g_{ij} = g_{ii} - g_{jj}$, amounting to $\Delta g^{P}_{xy} = 1.02 \times 10^{-3}$, $\Delta g^{P}_{yz} = 1.04 \times 10^{-3}$ for polarons,[33,47,48] and $\Delta g^{mF}_{xy} = 1.43 \times 10^{-4}$, $\Delta g^{mF}_{yz} = 1.83 \times 10^{-3}$ for methanofullerene radical anions.[33,48,49] The principal y-axis is chosen parallel to the longest P3DDT c-axis, and the x-axis lies in the thiophene rings plane. The z-axis is perpendicular to both x- and y-axes as seen in Figure 3.

Figure 3 shows also a typical spectrum calculated in this way together with its terms due to localized polarons and methanofullerene radical anions, $P^{+\bullet}_{loc}$ and $mF^{-\bullet}_{loc}$, respectively, with weakly anisotropic magnetic resonance parameters captured by spin traps as well as due to their mobile pairs of oppositely charged carriers $P^{+\bullet}_{mob} \leftrightarrow mF^{-\bullet}_{mob}$. It should be noted that paramagnetic centers immobilized by spin traps also take part in charge transport, however, indirectly. Magnetic resonance parameters used for the calculation of spectral contributions of these charge carriers are summarized in Table 3. They lie close to those obtained for analogous radicals photoinduced in other fullerene-modified conjugated polymers, including P3DDT.[27,50−52] Once the spin motion is accelerated

https://doi.org/10.1021/acs.jpcc.1c10407
J. Phys. Chem. C 2022, 126, 4495−4507

Table 3. Magnetic Resonance Parameters of Charge Carriers Used for Calculation of LEPR Spectra of the Initial and Acene-Modified Composites[a]

parameter	P3DDT:$PC_{61}BM$	P3DDT:$PC_{61}BM$/$NP_{0.06}$	P3DDT:$PC_{61}BM$/$AN_{0.06}$
g^{P}_{iso}	2.001_{85}	2.001_{90}	2.001_{92}
g^{mF}_{iso}	1.999_{86}	1.999_{85}	1.999_{87}
ΔB^{P}_{iso}, mT	0.175	0.178	0.171
ΔB^{mF}_{iso}, mT	0.105	0.103	0.095
n^{mF}_{mob}/n^{P}_{loc}	0.639	0.693	0.301
ω^{c}_{P}, eV	0.64	0.44	0.63
E^{c}_{P}, eV	1.63	1.66	1.64
ω^{c}_{mF}, eV	0.45	0.54	0.57
E^{c}_{mF}, eV	2.72	2.98	3.06

[a]Steady-state irradiated by the white light with color temperature T_c = 5000 K at the internal magnetic field of B_0 = 334 mT and T = 77 K. The concentration parameters, ω^{c}_{P}, E^{c}_{P}, ω^{c}_{mF}, and E^{c}_{mF}, determined from eq 2 are also presented.

magnetic resonant anisotropy of charge carriers is leveled due to the exchange of contributions of their spins differently oriented in an external magnetic field. The line width of charge carriers characterizing their spin state may consist of different contributions originating due to mutual interaction with environmental mobile and/or immobilized electron and nuclear spins:

$$\Delta B^{i}_{pp} = \Delta B^{(0)}_{pp} + \Delta B^{dyn}_{pp} + \Delta B^{gs}_{pp} \quad (1)$$

where $\Delta B^{(0)}_{pp}$ is a secular term reflecting hyperfine spin interaction (hfi) with other spin ensembles, whereas the frequency-dependent terms ΔB^{dyn}_{pp} and ΔB^{gs}_{pp} appear due to radical vibration/libration and hopping dynamics as well as g-strain in a disordered system, respectively. The g-strain originates in the Gaussian form of the respective term of eq 1 that becomes most noticeable at millimeter waveband LEPR.[34] The analysis of LEPR data obtained for the analogous charge carriers excited in the P3HT:$PC_{61}BM$ BHJ at a wide MW frequency range[53] allowed to postulate the last factor to be prevalence to the effective broadening of polymer:methanofullerene millimeter waveband LEPR spectra. Extrapolation to the $\omega_e \to 0$ limit gives line widths, $\Delta B^{(0)}_{pp}$ = 0.101 and 0.066 mT, is typical for these charge carriers in such systems. This makes it possible to determine separate spin−spin transverse relaxation times T_2 for both spin charge carriers (see below). The fitting of the samples under study demonstrated the Lorentzian shape of the total X-band LEPR spectra, including its contributions, so it can be assumed that the second term of eq 1 mainly reflects the mobility of spin charge carriers in polymer systems.[54,55]

3.3. Concentration of Spin Charge Carriers Photoinitiated in the Samples. An effective spin concentration is another important parameter, registering in the samples steady-state illuminated under study by the LEPR method. In general, it is a balance/difference number of spins, photoinitiated and recombined in the BHJ border. It should to reflect the quantum yield, the stability of charge carriers, and, as a result, the PCE of the photovoltaic system. There are many domestic and external factors affecting the excitation of such spins. For example, it may be the composition, structure, morphology of the BHJ, concentration, distribution, and energy depth of spin traps forming in a polymer matrix, as well as the temperature and energy of excited light photons. Spin susceptibility of polymer composites is governed also by their treatment by different additives that change the above properties.

The Figure 4 demonstrates how changes the n_{eff} parameter obtained for spin charge carriers steady-state excited by the white light with a color temperature T_c = 5000 K in the initial P3DDT:$PC_{61}BM$ composite upon its doping up to the level of y = 0.06 by π-conjugated acenes with different phenyl circles N_{ph}. It is seen from the figure that the introduction of a trace number of small planar naphthalene molecules into the composite bulk leads to a sharp increase in this parameter. However, the concentration of paramagnetic centers decreases monotonically down approximately to the initial value upon the doping of the composite by additives with a large number of phenyl cycles N_{ph}. At the same time, the number of light photons absorbed by the acene-modified sample grows with an increase in this parameter (see the inset in Figure 2). The LUMO and HOMO energies of molecular orbitals and band gap of the acenes used in experiments were calculated using the Orca program with the RHF SP functional and def2-SVP basis set and are summarized in Table 2. The energies E_g of band gap of polycyclic aromatic hydrocarbons as well as exemplary spin density isosurface plot of NP are also shown in Figure 4. The analysis of the data obtained allow us to conclude a direct dependence of the concentration of spin charge carriers photoexcited in the weakly doped composite from the band gap of additives introduced in its bulk. It is seen clearly that spin concentration experimentally obtained for the composite follows the respective dependence calculated for the acenes' band gap energy. For comparison, the same parameters determined for these acenes by Mekenyan et al.[38] are also depicted in the Figure 4. From the analysis of the data presented, a note should be made regarding some their scattering. Generally, quantum chemical calculations are carried out using various algorithms and approaches that determine their accuracy. Besides, they should consider the influence of possible effects affecting the final result. For example, the value of band gap calculated for isolated benzene molecule by different

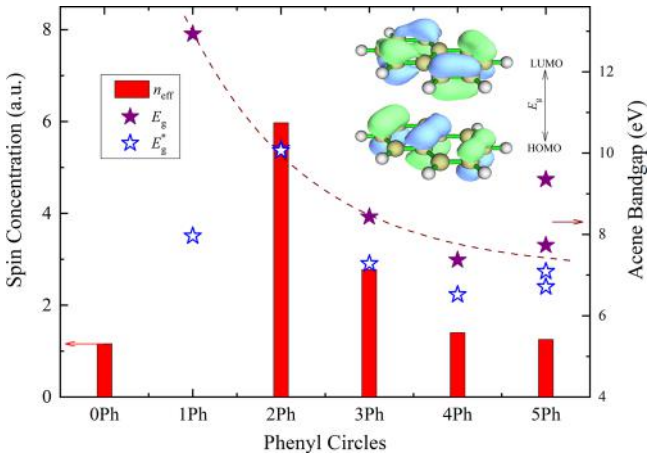

Figure 4. Effective concentration n_{eff} of spins excited in the initial P3DDT:$PC_{61}BM$ composite without phenyl molecules (N_{ph} = 0) and BHJ doped with naphthalene (NP, N_{ph} = 2), anthracene (AN, N_{ph} = 3), tetracene (TC, N_{ph} = 4), and perylene (PE, N_{ph} = 5) up to the level y = 0.06 illuminated by photons of the white light at T = 77 K. The filled and open stars show the band gap energy $E_g = E_{LUMO} - E_{HOMO}$ calculated for the acenes used in the present work in comparison with those reported by Mekenyan et al.[38] Exemplary LUMO and HOMO molecular orbitals calculated for naphthalene are also depicted. The dashed line shows the dependence calculated using $E_g \propto 7.38/N_{ph}$.

https://doi.org/10.1021/acs.jpcc.1c10407
J. Phys. Chem. C 2022, 126, 4495−4507

methods can vary within 5.12−10.5 eV;[16,38,56,57] however, its optical gap was measured to be around 3.6 eV,[58] due to the effect of large exciton binding in small molecules equal, e.g., for this molecule 3.10 eV.[59] Nevertheless, the data obtained allows us to hypothesize a close relationship of electronic properties of a composite with the band structure of an acene. Indeed, Figure 4 evidence that they follow a $E_g \propto 7.38/N_{ph}$ dependence typical for polycyclic aromatic hydrocarbons.[60] To confirm this supposition, it would be important to obtain also respective correlations of magnetic resonant, spin and dynamic parameters of mobile and localized charge carriers with molecular and structural properties of the initial and doped composites, as well as with the exciting photon energy. It should also to analyze a possible formation of localized polaron pairs $P^{+\bullet}_{loc} \leftrightarrow P^{-\bullet}_{loc}$ with equal energetic and magnetic resonant parameters[61] as well as diamagnetic bipolarons each potentially dissociating into spin polaron couples, $BP^{2+} \leftrightarrow 2P^{+\bullet}$ in polymer composite matrices,[62,63] including P3DDT.[64] Some charge carriers captured by spin traps can also be released from the latter when interacting with light photons of a certain energy. The combination of these processes could supply principally unusual information in the study of spin-assisted magnetic resonance, relaxation, and dynamics processes carried out in polymer:-fullerene systems.

Below are presented the results of a detailed study of the mentioned properties of charge carriers excited by various light photons in the as-prepared composite P3DDT:$PC_{61}BM$, as well as in its BHJ, weakly modified by naphthalene and anthracene molecules, P3DDT:$PC_{61}BM/NP_{0.06}$ and P3DDT:$PC_{61}BM/AN_{0.06}$, respectively. The interpretation of electronic properties of organic polymer composites was shown[27,65] to become more precise and simpler analyzing the concentration ratio of mobile and localized charge carriers, $n^{P,mF}_{mob}/n^{P}_{loc}$, which is less sensitive to various factors affecting their magnetic and electronic properties. These parameters obtained for the samples under study steady-state irradiated by a white light source with a color temperature T_c = 5000 K are also presented in Table 3. The higher this ratio, the faster the charge transfer in the BHJ; therefore, the better PCE should be reached for such a photovoltaic system. Figure 5 depicts such parameters determined for the mobile and captured polarons and methanofullerene radical anions photoinitiated in the above-mentioned samples. Upon inspecting Figure 5, it is clear that the ratio $n^{P,mF}_{mob}/n^{P}_{loc}$ is sensitive not only to the structural properties of a composite but also to the energy of exciting light photons. As seen from the figure, all the samples demonstrate extreme dependences of the ratio on the energy of excited photons. Assuming a Gaussian distribution of paramagnetic centers excited in various areas of the disordered composites, these curves can be approximated by a two-term equation:

$$A = \frac{A^0_P}{\omega^c_P}\exp\left[-2\left(\frac{E_{ph}-E^c_P}{\omega^c_P}\right)^2\right] + \frac{A^0_{mF}}{\omega^c_{mF}}\exp\left[-2\left(\frac{E_{ph}-E^c_{mF}}{\omega^c_{mF}}\right)^2\right] \quad (2)$$

where $A \equiv n^{P,mF}_{mob}/n^{P}_{loc}$, the concentration trios A^0_P, ω^c_P, E^c_P and A^0_{mF}, ω^c_{mF}, E^c_{mF}, are the coefficients, widths, and extremum energies characteristic for polarons and methanofullerene radical anions, respectively. Both last parameters determined for the samples from experimental data depicted in the figure are also presented in Table 3.

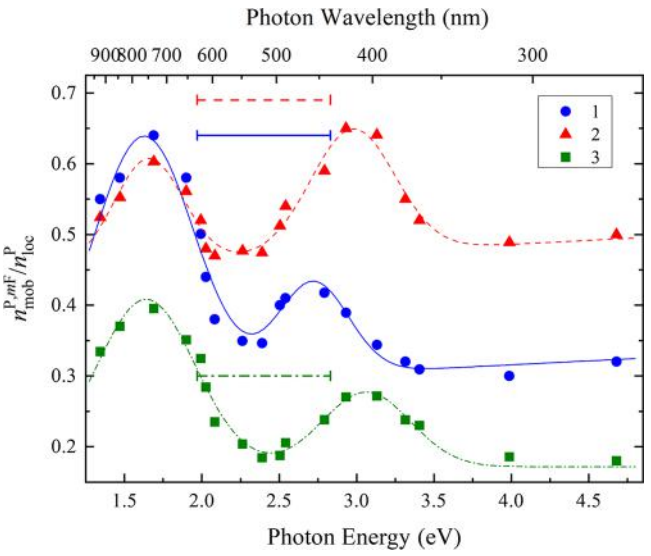

Figure 5. Concentration ratio $n^{P,mF}_{mob}/n^{P}_{loc}$ obtained for the composite P3DDT:$PC_{61}BM$ before (1) and after doping up to level y = 0.06 with naphthalene, P3DDT:$PC_{61}BM/NP_{0.06}$ (2), and anthracene, P3DDT:$PC_{61}BM/AN_{0.06}$ (3), respectively, upon steady-state illumination as a function of photon energy $h\nu_{ph}$. The corresponding parameters obtained for the samples illuminated by white light with color temperature of T_c = 5000 K are shown by horizontal solid, dashed, and dashed and dotted spectral half-height sections, respectively. Two-term dependencies, calculated from eq 2 with respective concentration parameters ω_i and E_j in Table 2 obtained for polarons and methanofullene radical anions, are also shown.

It is seen from the Figure 5 that the concentration dependence of the initial sample can be described by at least two extremes near $h\nu_{ph}$ = 1.63 and 2.72 eV that is close to the respective band gaps of electron-donating and -accepting moieties, respectively. The low-energy extremum does not shift noticeably after modification of as-prepared composite by NP or AN, whereas its second extremum shifts to 2.98 eV and then to 3.06 eV, respectively, as a result of such procedure. Such transformations can be explained by the higher exchange interaction of the methanofullerene radical anions and these additives with planar and extended $\pi-\pi^*$-structure. In this case, the NP and AN molecules introduced into the bulk of the initial composite act as the centers for its structuring as it happens in such backbone modified by other small 2D molecules.[27] A greater increase in sum concentration of paramagnetic centers and the A value is obtained for the NP-modified second composite. This evidence greater efficiency of the polymorphic transition, as well as the better stability of excited charge carriers.

3.4. Relaxation and Dynamics of Spin Charge Carriers Photoexcited in the Composites. Organic radicals formed in photovoltaic systems registered at an internal magnetic field $B_0 \leq 0.33$ T far enough from MW saturation regime are characterized by homogeneous Lorentzian line with a width of $\Delta B^{(L)}_{pp}$. This makes it possible to determine separately the spin−spin transverse relaxation times T_2 for both spin charge carriers from the following equation:[55]

$$T_2 = \frac{2}{\sqrt{3}\gamma_e \Delta B^{(L)}_{pp}} \quad (3)$$

https://doi.org/10.1021/acs.jpcc.1c10407
J. Phys. Chem. C 2022, 126, 4495−4507

where γ_e is the electron gyromagnetic ratio. Longitudinal relaxation times T_1 can be estimated from the classical analysis of spectral saturation of homogeneously broadened lines with amplitude I:[66,67]

$$I = I_0 B_1 \left(1 + \frac{2\gamma_e B_1^2 T_1}{\sqrt{3}\,\Delta B_{pp}^{(0)}}\right)^{-3/2} \quad (4)$$

where I_0 is the amplitude of nonsaturated line registered far from MW saturation conditions and B_1 is the magnetic term of the MW field. Since both charge carriers are characterized by different magnetic resonance and relaxation parameters, the above-mentioned procedure allows one to determine both their relaxation times. Figure 6 exhibits exemplary intensities of

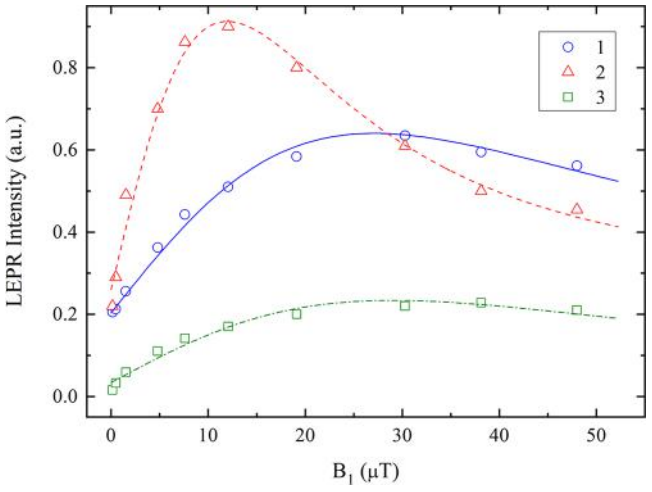

Figure 6. Intensity of LEPR terms of localized polarons $P_{loc}^{+\bullet}$ (1), mobile polarons $P_{mob}^{+\bullet}$ (2), and localized methanofullerene radical anions $mF_{loc}^{-\bullet}$ (3) photoinitiated in the initial P3DDT:PC_{61}BM BHJ by photons with the energy/wavelength of 2.03/612 eV/nm at different MW power magnetic terms, B_1. The respective lines calculated from eq 3 $T_1 = 5.12 \times 10^{-7}$, 1.98×10^{-6}, and 3.13×10^{-7} s are shown by solid, dashed, and dashed and dotted lines.

localized and mobile spin charge carriers photoinitiated in nonmodified composite P3DDT:PC_{61}BM as a function of the B_1 value. It is seen from the figure that the dependence $I(B_1)$ obtained for mobile charge carriers starts to deviate from linear at smaller B_1 as compared to that determined for charge carriers captured by spin traps. This can occur due to greater isolation of positively charged polarons photoexcited on conjugated P3DDT chains by side substituents, which prevents their interaction with the nearest spin environment and, therefore, their transition to a ground state. In this regard, it should be noted that a relatively opposite saturation regime registered for the same charge carriers initiated in the P3HT:PC_{61}BM composite with shorter lateral substituents,[51] so both relaxation times of different spin ensembles were determined separately in their steady-state MW saturation regime according to the approach proposed for conjugated systems.[55]

Figure 7 depicts both relaxation times T_1 and T_2 determined by the above-mentioned procedure for localized and mobile charge carriers initiated in P3DDT:PC_{61}BM, P3DDT:PC_{61}BM/$NP_{0.06}$, and P3DDT:PC_{61}BM/$AN_{0.06}$ BHJ at T = 77 K and varying initiating photon energy $h\nu_{ph}$ within the region of 1.34−4.52 eV. The same parameters obtained for these samples illuminated by white light with T_c = 5000 K are summarized in Table 3. From the analysis of the dependencies presented, some conclusions can be made. The first of these is the variation of spin relaxation with the photon energy, which however become stronger than that obtained for structurally related P3HT:PC_{61}BM composite.[68] The second is the obviously extreme nature of the dependences obtained for spin−lattice relaxation in the samples specified. Similar dependencies obtained for other polymer:fullerene systems are characterized by variant-specific extremes.[27,28,65] Most of the dependencies shown in Figure 7 are characterized by at least two extremes. Analogous to the above-mentioned spin concentration dependences, they can also be approximated by eq 2 with $A \equiv T_1^{P,mF}$ obtained for both mobile spin charge carriers excited in the samples under study and the respective mating relaxation parameters ω_p^r, E_p^r and ω_{mF}^r, E_{mF}^r summarized in Table 3. The low-energy term can also be attributed to the band structure of its polymer matrix. Lying initially near $h\nu_{ph}$ = 1.78 eV, it shifts to 2.12 eV and returns nearly to the initial value upon its modification with the NP and AN molecules, respectively. The position of the second extremum, initially registered near $h\nu_{ph}$ = 2.39 eV, shifts to 3.03 eV, and comes partly back to 2.73 eV as a result of such composite treatment (see Figure 7). This may occur due to the sensitivity of methanofullerene radical anions to specific light photons or/and the presence of small molecular additives both of which affect the composite band gap. The half-height width of these contributions is significantly higher than those of the initial and treated polymer matrices. This should indicate a differently distributed interaction of methanofullerene spins with microenvironment in disordered samples. It should be emphasized that a significant decrease in the extremality of respective dependencies obtained for the composite P3DDT:PC_{61}BM/$NP_{0.06}$ (see Figure 7b). A longer spin−lattice relaxation of both mobile charge carriers is consistent

Electron relaxation of spin charge carriers is governed also by their dynamics. Spin dynamics induces an additional magnetic field, which accelerates electron relaxation of both spin ensembles stabilized in BHJ. Assuming polaron translative hopping along and between P3DDT chains with respective diffusion coefficients D_{1D} and D_{3D}, respectively, and vibrational/librational mobility of methanofullerene molecules around their own main axis with diffusion coefficient D_v, one can write the equations interconnecting relaxation and dynamic parameters of paramagnetic centers with spin S = 1/2 as[69,70]

$$T_1^{-1}(\omega_e) = \langle\omega^2\rangle[2J(\omega_e) + 8J(2\omega_e)] \quad (5)$$

$$T_2^{-1}(\omega_e) = \langle\omega^2\rangle[3J(0) + 5J(\omega_e) + 2J(2\omega_e)] \quad (6)$$

where $\langle\omega^2\rangle = 1/10\gamma_e^4\hbar^2 S(S+1)\, n\Sigma_{ij}$ is a constant of a dipole−dipole interaction for powder-like sample with n localized and mobile spins per monomer unit and lattice sum Σ_{ij}, $J(\omega_e) = (2D_\parallel^{1D}\omega_e)^{-1/2}$ at $D_\parallel^{1D} \gg \omega_e \gg D_{3D}$ or $J(0) = (2D_\parallel^{1D}D_{3D})^{-1/2}$ at $D_{3D} \gg \omega_e$ is a spectral density function for quasi-one-dimensional (Q1D) motion,[71,72] $D_\parallel^{1D} = 4D_{1D}/L^2$, ω_e is resonant angular frequency of electron spin precession, and L is the spatial extent of the polaron wave function equivalent approximately to 4−5 monomer units for organic conjugated polymers, including regioregular P3HT and P3DDT.[73,74] A spectral density function for vibrational diffusion with correlation time τ_c is $J_v(\omega_e) = 2\tau_c/(1 + \tau_c^2\omega_e^2)$.

It was shown[28] that the polymorphic transition of copolymer BHJ with methanofullerene and nonfullerene acceptors accelerates spin interlayer hopping and increases the stability of both $\pi-\pi$-interacting charge carriers. This process should,

https://doi.org/10.1021/acs.jpcc.1c10407
J. Phys. Chem. C 2022, 126, 4495−4507

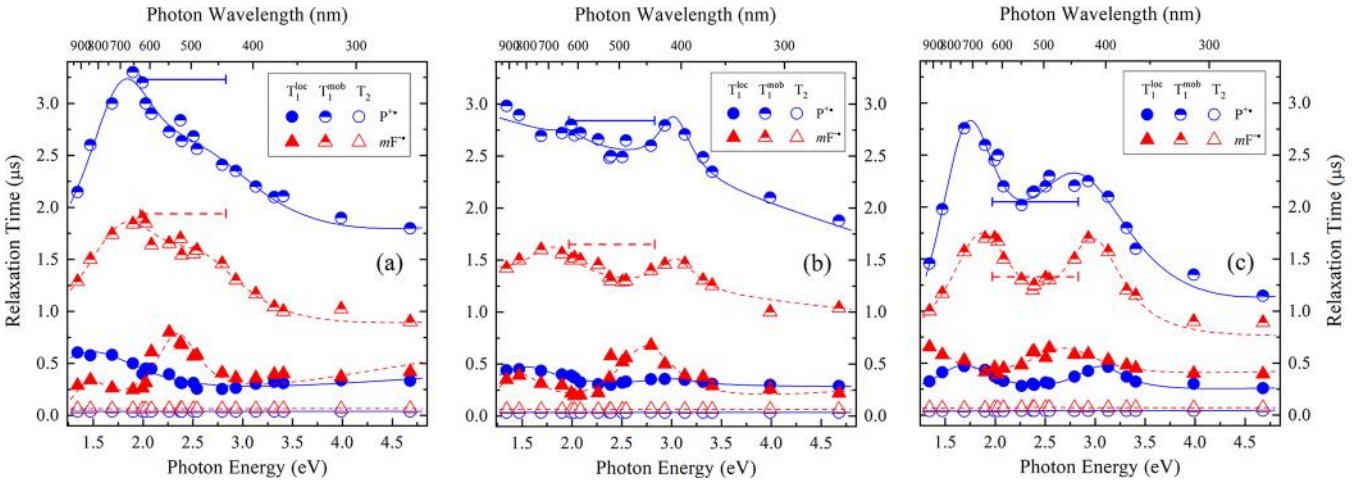

Figure 7. Spin−lattice T_1 and spin−spin T_2 relaxation times of localized and mobile polarons $P^{+\bullet}$ (*1*), localized and mobile methanofullerene radical anions $mF^{-\bullet}$ (*2*) photoinitiated in the composite P3DDT:$PC_{61}BM$ before (a) and after its doping with naphthalene (b) and anthracene (c) molecules up to the level of $y = 0.06$ illuminated at $T = 77$ K as a function of photon energy $h\nu_{ph}$. The corresponding T_1 values obtained for mobile polarons $P^{-\bullet}_{mob}$ and methanofullerene radical anions $mF^{-\bullet}_{mob}$ excited in these samples by white light with a color temperature of $T_c = 5000$ K are shown by horizontal solid and dashed spectral half-height sections, respectively. Two-term dependencies are also shown (calculated from eq 2 with respective concentration parameters ω_i and E_j in Table 2 obtained for mobile polarons and methanofullerene radical anions). The other dashed are drawn arbitrarily only for illustration to guide the eye.

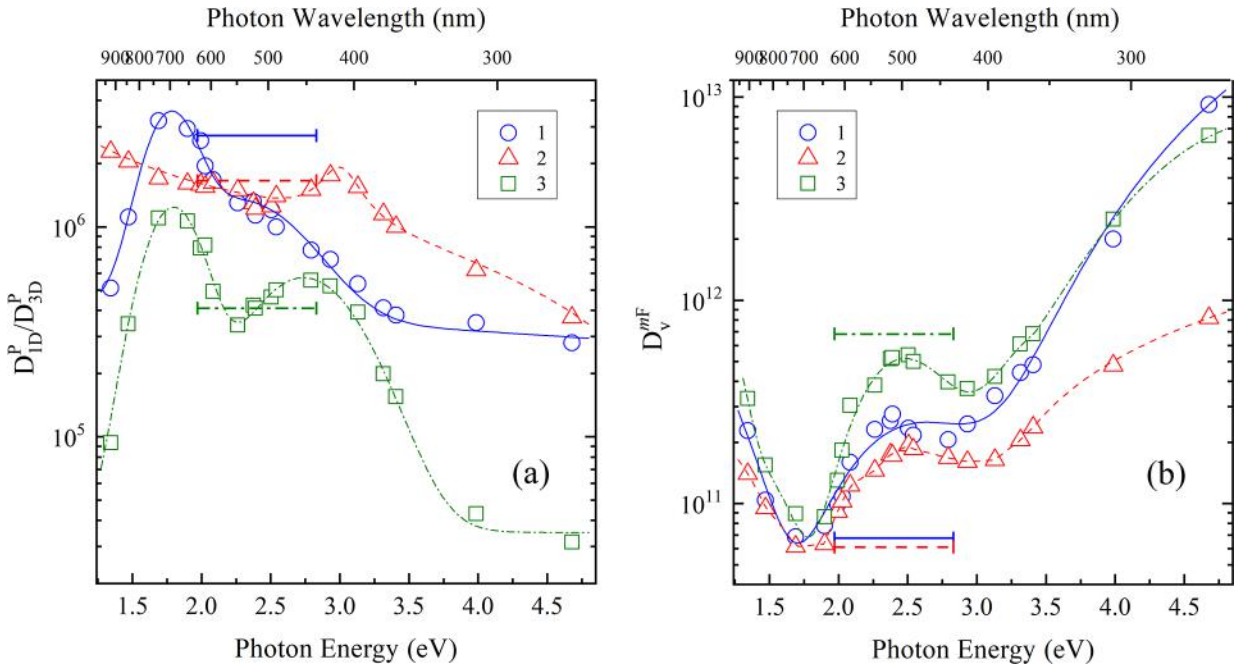

Figure 8. Anisotropy of polaron dynamics D^P_{1D}/D^P_{3D} (a) and coefficient of vibrational/librational diffusion D^{mF}_v of methanofullerene radical anions $mF^{-\bullet}_{mob}$ (b) photoinitiated in the composite P3DDT:$PC_{61}BM$ before (1) and after its doping with naphthalene (2) and anthracene (3) molecules up to the level of $y = 0.06$ at $T = 77$ K and different photon energy $h\nu_{ph}$. The corresponding values obtained for these samples illumined by white light with a color temperature of $T_c = 5000$ K are shown by horizontal solid, dashed, and dashed and dotted spectral half-height sections, respectively. Two-term dependencies are also shown (calculated from eq 2 with respective concentration parameters ω_i and E_j in Table 2 obtained for mobile polarons). The other dashed are drawn arbitrarily only for illustration to guide the eye.

therefore, be reflected in the anisotropy of polaron dynamics D^P_{1D}/D^P_{3D} in a composite. It means the higher this ratio, the greater the predominance of intrachain polaron 1D-mobility and the higher its sensitivity to the change in the system band gap and energy of photons, initiating such a change in the α-phase of disordered composite. In contrast, the decrease of this parameter should indicate the higher dimensionality/ordering of the system due to polymorphic $\alpha-\beta$-transition. This process should obviously be controlled by its unalterable modification by small 2D molecules or/and reversible variation of energy of the initiating photons. It would be quite important to note that the mobile radical anion $mF^{-\bullet}_{mob}$ could be used not only as an electron acceptor but also as a spin-probe-sensing property of its own microenvironment. In the other words, the more volume occupied by such a radical, the easier its vibrational dynamics.

Figure 8 demonstrates how the parameters D^P_{1D}/D^P_{3D} and D^{mF}_v changed, as obtained from eqs 5 and 6, for polarons and methanofullerene radical anions, respectively, excited in the

https://doi.org/10.1021/acs.jpcc.1c10407
J. Phys. Chem. C 2022, 126, 4495−4507

P3DDT:$PC_{61}BM$, P3DDT:$PC_{61}BM/NP_{0.06}$, and P3DDT:$PC_{61}BM/AN_{0.06}$ composites when varying irradiating their BHJ photon energy $h\nu_{ph}$. These parameters obtained for the samples illuminated by a white light source with T_c = 5000 K are also shown by respective linear segments and summarized in Table 3. The figure evidence an expectedly extreme character of these dependencies with at least two specific photon energies (except the NP-modified composite with the only extremum of the polaron dynamic parameter). The first of them is situated at $h\nu_{ph} \approx 1.8$ eV, which is close to the band gap of P3DDT. The position and amplitude of the second, high-energy extremes depend on the treatment of the sample. As in the case of concentration and relaxation data, the experimental results shown in Figure 8 should also follow a two-term equation (eq 2) with $A \equiv D^{P}_{1D}/D^{P}_{3D}$ and the respective parameters ω_i and E_j characteristic for polarons and methanofullene radical anions presented in Table 4. The anisotropy coefficient D^{P}_{1D}/D^{P}_{3D} of the initial sample reaches maxima at $h\nu_{ph}$ = 1.77 and 2.29 eV (Figure 8a). Once the sample is modified by NP molecules, the low-energy extreme nearly disappears, while the second extremum of dependence is shifted to $h\nu_{ph}$ = 3.01 eV. The AN-doping of composite weakly changes the position of the low-energy extremum; however, it shifts the second extreme to $h\nu_{ph}$ = 2.74 eV. The data obtained were interpreted in favor of improving the morphology of the NP-doped sample and increasing the dimensionality of polaron dynamics, so the modification with acene molecules provokes transition of its α-polymorph into a more ordered and higher dimensional β-phase. Such a transition becomes more probable when naphthalene molecules are introduced into the composite BHJ. This negates the sensitivity of dynamic parameters to the energy and density of exciting light photons and, thus, increases its quantum yield. If charged polarons hopping along the chaotically oriented chains of the initial composite, then the interlayer charge transfer becomes predominant in BHJ modified by acenes with a high band gap. Figure 8b demonstrates the effect of the photon energy on the value and positions of vibration coefficient D^{mF}_{v} of methanofullerene radical anions in the initial and acene-doped composites. It evidence approximately the opposite course of all energetic dependencies obtained for mobile radical anions $mF^{-\bullet}_{mob}$. It indicates a more inhibited dynamics of these charge carriers in the P3DDT:$PC_{61}BM/NP_{0.06}$ composite upon its irradiation by different light photons. This additionally testifies in favor of a more ordered structure of this compound with reduced interlayer distances.

Table 4. Relaxation and Dynamics Parameters of Charge Carriers[a]

parameter	P3DDT:$PC_{61}BM$	P3DDT:$PC_{61}BM$/$NP_{0.06}$	P3DDT:$PC_{61}BM$/$AN_{0.06}$
T_1^{Ploc}, s	1.52×10^{-6}	1.02×10^{-6}	2.23×10^{-7}
T_1^{Pmob}, s	3.24×10^{-6}	2.84×10^{-6}	2.05×10^{-6}
T_1^{mFmob}, s	1.94×10^{-6}	1.65×10^{-6}	1.33×10^{-6}
T_1^{mFloc}, s	2.65×10^{-7}	3.94×10^{-7}	1.97×10^{-7}
T_2^{P}, s	3.74×10^{-8}	3.69×10^{-8}	3.84×10^{-8}
T_2^{mF}, s	6.24×10^{-8}	6.36×10^{-8}	6.91×10^{-8}
ω^{r}_{P}, eV	0.52	0.61	0.49
E^{r}_{P}, eV	1.78	2.12	1.72
ω^{r}_{mF}, eV	1.23	0.40	1.14
E^{r}_{mF}, eV	2.39	3.03	2.73
D^{P}_{1D}, rad/s	1.16×10^{12}	1.36×10^{12}	1.04×10^{12}
D^{P}_{3D}, rad/s	3.89×10^{5}	4.90×10^{5}	1.03×10^{6}
D^{mF}_{v}, rad/s	6.76×10^{10}	6.10×10^{10}	1.18×10^{11}
D^{P}_{1D}/D^{P}_{3D}	2.72×10^{6}	1.66×10^{6}	4.10×10^{5}
ω^{d}_{P}, eV	0.34		0.39
E^{d}_{P}, eV	1.77		1.79
ω^{d}_{mF}, eV	0.84	0.28	0.76
E^{d}_{mF}, eV	2.29	3.01	2.74

[a]Steady-state initiated by the white light with color temperature T_c = 5000 K in the initial and acene-modified composites at T = 77 K. The relaxation, ω^{r}_{P}, E^{r}_{P}, ω^{r}_{mF}, and E^{r}_{mF}, and dynamics, ω^{d}_{P}, E^{d}_{P}, ω^{d}_{mF}, and E^{d}_{mF}, parameters determined from eq 2 for mobile paramagnetic centers are also presented.

CONCLUSION

Relaxation, magnetic resonance, and dynamics properties of spin charge carriers photoinitiated in the initial P3DDT:$PC_{61}BM$ composite were studied by a direct LEPR method. The main properties of positively charged polarons and oppositely charged methanofullerene radical anions were shown to be determined by the structure and morphology of this photovoltaic system, spin traps formed in its disordered matrix, and the density and energy of the initiating light photons. These parameters can be also changed by adding into the P3DDT:$PC_{61}BM$ BHJ a percentage of small 2D molecules with an extended π-structure. It was found that small planar acene molecules being added into the initial composite solution indirectly pull together the nearest macromolecules rather than the role of crystallization centers analogous to that as it occurs upon launching of the boiling process in liquids or growth of common solid crystals. A calculations of the acenes' band structure allows us to point out a close relationship of their band gap and spin-assisted properties of modified composite. The rate of a restructuring process carried out during the preparation of the samples appeared to be inversely proportional to the acene band gap. This allows us to conclude that such a triggerlike phase transitions lead to a significant decrease in the number of spin traps, as well as increases in stability and concentration of spin charge carriers and their interaction with the lattice environment. The slight treatment of the initial composite with the simplest polycyclic aromatic hydrocarbons increases its ordering/crystallinity due to polymorphic $\alpha-\beta$-transition in polymer matrix with reduced distances between layered stacks. The enhanced $\pi-\pi$ interaction provokes higher overlapping of the wave functions of polymer chains and nearest additives, accelerates electron relaxation of all spin ensembles formed in the systems under study, decreases a number of spin traps, and broadens their high-energy optical absorption band. Eventually, it increases the stability of spin charge carriers photoinitiated in a composite doped with anthracene or naphthalene molecules in more than 2 or 5 fold, respectively. This eliminates the selectivity of spin charge carriers to the photon energy and changes in the mechanism of their transfer toward the electrodes. If the charge is transferred mainly by polarons along the polymer chains in an amorphous α-phase of a composite, then its hopping between the 2D-layered stacks prevails in its more crystalline β-polymorphs. Polymorphism and modification of organic polymer:fullerene allows a shift of the balance of their metastable amorphous α-phase toward the more stable and crystalline β-polymorph. This can be realized either by an irreversible triggerlike modification of the composite with small planar molecules with extended $\pi-\pi$ structure or/and its episodic treatment by certain light photons. The spin-assisting character of the relaxation and dynamics processes carried out in the initial and slightly modified BHJ was shown. This allows significant acceleration of the transfer of

https://doi.org/10.1021/acs.jpcc.1c10407
J. Phys. Chem. C 2022, 126, 4495−4507

charge carriers through BHJ, increasing their stability and thereby improving functionality and energy-conversing efficiency of the system. The obtained results serve to strengthen a universal proposal of using optimally acene-doped polymers and their fullerene-modified composites for the creation of electronic and spintronic devices with spin-photon-assisted parameters. The method proposed can be used also for analogous research of other organic donor−acceptor systems with spin charge dynamics.

AUTHOR INFORMATION

Corresponding Author

Victor I. Krinichnyi − *Department of Kinetics and Catalysis, Institute of Problems of Chemical Physics RAS, Chernogolovka 142432, Russia*; orcid.org/0000-0002-5227-763X; Email: kivi@icp.ac.ru, kivirus@gmail.com

Authors

Evgeniya I. Yudanova − *Department of Kinetics and Catalysis, Institute of Problems of Chemical Physics RAS, Chernogolovka 142432, Russia*

Nikolay N. Denisov − *Department of Kinetics and Catalysis, Institute of Problems of Chemical Physics RAS, Chernogolovka 142432, Russia*

Complete contact information is available at: https://pubs.acs.org/10.1021/acs.jpcc.1c10407

Author Contributions

The manuscript was written through contributions of all authors. All authors have given approval to the final version of the manuscript.

Notes

The authors declare no competing financial interest.

ACKNOWLEDGMENTS

This work was carried out with financial support from the Russian Foundation for Basic Research, Grant No. 18-29-20011-mk according to the State Assignment No. AAAA-A19-119032690060-9.

REFERENCES

(1) Baranovskii, S. D.; Rubel, O.; Jansson, F.; Österbacka, R. *Organic Electronics*; Springer-Verlag: Berlin Heidelberg, 2010; Vol. *223*, p 328.

(2) Huang, F.; Yip, H.-L.; Cao, Y. *Polymer Photovoltaics: Materials, Physics, and Device Engineering*; The Royal Society of Chemistry: Cambridge, U.K., 2015; p 406.

(3) Khalifeh, S. *Polymers in Organic Electronics. Polymer Selection for Electronic, Mechatronic, and Optoelectronic Systems*; ChemTec Publishing: Toronto, 2020.

(4) Steyrleuthner, R.; Di Pietro, R.; Collins, B. A.; Polzer, F.; Himmelberger, S.; Schubert, M.; Chen, Z. H.; Zhang, S. M.; Salleo, A.; Ade, H.; et al. The Role of Regioregularity, Crystallinity, and Chain Orientation on Electron Transport in a High-Mobility N-Type Copolymer. *J. Am. Chem. Soc.* **2014**, *136*, 4245−4256.

(5) Steyrleuthner, R.; Schubert, M.; Howard, I.; Klaumünzer, B.; Schilling, K.; Chen, Z.; Saalfrank, P.; Laquai, F.; Facchetti, A.; Neher, D. Aggregation in a High-Mobility N-Type Low-Bandgap Copolymer with Implications on Semicrystalline Morphology. *J. Am. Chem. Soc.* **2012**, *134*, 18303−18317.

(6) Li, M.; Balawi, A. H.; Leenaers, P. J.; Ning, L.; Heintges, G. H. L.; Marszalek, T.; Pisula, W.; Wienk, M. M.; Meskers, S. C. J.; Yi, Y.; et al. Impact of Polymorphism on the Optoelectronic Properties of a Low-Bandgap Semiconducting Polymer. *Nat. Commun.* **2019**, *10*, 2867.

(7) Zhang, Y.; Gautam, B. R.; Basel, T. P.; Mascaro, D. J.; Vardeny, Z. V. Organic Bulk Heterojunction Solar Cells Enhanced by Spin Interaction. *Synth. Met.* **2013**, *173*, 2−9.

(8) Poelking, C.; Andrienko, D. Effect of Polymorphism, Regioregularity and Paracrystallinity on Charge Transport in Poly(3-Hexylthiophene) P3HT Nanofibers. *Macromolecules* **2013**, *46*, 8941−8956.

(9) Panzer, F.; Sommer, M.; Bässler, H.; Thelakkat, M.; Köhler, A. Spectroscopic Signature of Two Distinct H-Aggregate Species in Poly(3-Hexylthiophene). *Macromolecules* **2015**, *48*, 1543−1553.

(10) Causin, V.; Marega, C.; Marigo, A.; Valentini, L.; Kenny, J. M. Crystallization and Melting Behavior of Poly(3-Butylthiophene), Poly(3-Octylthiophene), and Poly(3-Dodecylthiophene). *Macromolecules* **2005**, *38*, 409−415.

(11) Guo, Y.; Wang, L.; Han, Y. Y.; Geng, Y. H.; Su, Z. H. Influence of Molecular Weight on Polymorphs and Temperature-Induced Structure Evolution of Regioregular Poly(3-Dodecylthiophene). *Polym. Chem.* **2014**, *5*, 1938−1944.

(12) Ranzieri, P.; Girlando, A.; Tavazzi, S.; Campione, M.; Raimondo, L.; Bilotti, I.; Brillante, A.; Della Valle, R. G.; Venuti, E. Polymorphism and Phonon Dynamics of A-Quaterthiophene. *ChemPhysChem* **2009**, *10*, 657−663.

(13) Carati, C.; Gasparini, N.; Righi, S.; Tinti, F.; Fattori, V.; Savoini, A.; Cominetti, A.; Po, R.; Bonoldi, L.; Camaioni, N. Pyrene−Fullerene Interaction and Its Effect on the Behavior of Photovoltaic Blends. *J. Phys. Chem. C* **2016**, *120*, 6909−6919.

(14) Zhang, H.; Liu, Y.; Xu, B.; Chen, G.; Wang, C.; Wen, S.; Li, Y.; Liu, L.; Tian, W. Effects of DIO on the Charge Recombination Behaviors of PTB7:PC71BM Photovoltaics. *Org. Electron.* **2019**, *67*, 50−56.

(15) Noriega, R.; Rivnay, J.; Vandewal, K.; Koch, F. P. V.; Stingelin, N.; Smith, P.; Toney, M. F.; Salleo, A. A General Relationship between Disorder, Aggregation and Charge Transport in Conjugated Polymers. *Nat. Mater.* **2013**, *12*, 1038−1044.

(16) Masiak, P.; Wierzbowska, M. Ferroelectric Π-Stacks of Molecules with the Energy Gaps in the Sunlight Range. *J. Mater. Sci.* **2017**, *52*, 4378−4388.

(17) Meille, S. V.; Romita, V.; Caronna, T.; Lovinger, A. J.; Catellani, M.; Belobrzeckaja, L. Influence of Molecular Weight and Regioregularity on the Polymorphic Behavior of Poly(3-Decylthiophenes). *Macromolecules* **1997**, *30*, 7898−7905.

(18) Yuan, Y.; Zhang, J.; Sun, J.; Hu, J.; Zhang, T.; Duan, Y. Polymorphism and Structural Transition around 54 °C in Regioregular Poly(3-Hexylthiophene) with High Crystallinity as Revealed by Infrared Spectroscopy. *Macromolecules* **2011**, *44*, 9341−9350.

(19) Lu, G. H.; Li, L. G.; Yang, X. N. Achieving Perpendicular Alignment of Rigid Polythiophene Backbones to the Substrate by Using Solvent-Vapor Treatment. *Adv. Mater.* **2007**, *19*, 3594−3598.

(20) Prosa, T. J.; Winokur, M. J.; McCullough, R. D. Evidence of a Novel Side Chain Structure in Regioregular Poly(3-Alkylthiophenes). *Macromolecules* **1996**, *29*, 3654−3656.

(21) Dillon, A. C. Carbon Nanotubes for Photoconversion and Electrical Energy Storage. *Chem. Rev.* **2010**, *110*, 6856−6872.

(22) Min, J.; Kwon, O. K.; Cui, C.; Park, J.-H.; Wu, Y.; Park, S. Y.; Li, Y.; Brabec, C. J. High Performance All-Small-Molecule Solar Cells: Engineering the Nanomorphology Via Processing Additives. *J. Mater. Chem. A* **2016**, *4*, 14234−14240.

(23) Cominetti, A.; Pellegrino, A.; Longo, L.; Tacca, A.; Po, R.; Carbonera, C.; Salvalaggio, M.; Baldrighi, M.; Meille, S. V. Polymer Solar Cells Based on Fullerene-Pyrene Acceptor Systems. *Mater. Chem. Phys.* **2015**, *159*, 46−55.

(24) Chen, H.; Zhang, R.; Chen, X.; Zeng, G.; Kobera, L.; Abbrent, S.; Zhang, B.; Chen, W.; Xu, G.; Oh, J.; et al. A Guest-Assisted Molecular-Organization Approach for > 17% Efficiency Organic Solar Cells Using Environmentally Friendly Solvents. *Nature Energy* **2021**, *6*, 1045−1053.

(25) Krinichnyi, V. I. *Multi Frequency EPR Spectroscopy of Conjugated Polymers and Their Nanocomposites*; CRC Press Taylor & Francis Group: Boca Raton, FL, 2016; p 314.

(26) Krinichnyi, V. I. EPR Spectroscopy of Polymer:Fullerene Nanocomposites. In *Spectroscopy of Polymer Nanocomposites*; Thomas, S., Rouxel, D., Ponnamma, D., Eds.; Elsevier: Amsterdam, 2016; pp 202−275.
(27) Krinichnyi, V. I.; Yudanova, E. I.; Denisov, N. N.; Bogatyrenko, V. R. Effects of Small-Molecule-Doping on Spin-Assisted Processes in P3DDT:$PC_{61}BM$ Photovoltaics. *Synth. Met.* **2020**, *267*, 116462.
(28) Krinichnyi, V. I.; Yudanova, E. I.; Denisov, N. N.; Konkin, A. A.; Ritter, U.; Bogatyrenko, V. R.; Konkin, A. L. Light-Induced Electron Paramagnetic Resonance Study of Charge Transport in Fullerene and Nonfullerene PBDB-T-Based Solar Cells. *J. Phys. Chem. C* **2021**, *125*, 12224−12240.
(29) Tashiro, K.; Ono, K.; Minagawa, Y.; Kobayashi, M.; Kawai, T.; Yoshino, K. Structure and Thermochromic Solid-State Phase-Transition of Poly(3-Alkylthiophene). *J. Polym. Sci., Part B* **1991**, *29*, 1223−1233.
(30) Sensfuss, S.; Al-Ibrahim, M. Optoelectronic Properties of Conjugated Polymer/Fullerene Binary Pairs with Variety of Lumo Level Differences. In *Organic Photovoltaics: Mechanisms, Materials, and Devices (Optical Engineering)*; Sun, S. S., Sariciftci, N. S., Eds.; CRC Press: Boca Raton, FL, 2005; pp 529−557.
(31) Sensfuss, S.; Al-Ibrahim, M.; Konkin, A.; Nazmutdinova, G.; Zhokhavets, U.; Gobsch, G.; Egbe, D. A. M.; Klemm, E.; Roth, H. K. Characterization of Potential Donor Acceptor Pairs for Polymer Solar Cells by ESR, Optical, and Electrochemical Investigations. *Proc. Opt. Sci. Technol.* **2003**, 129−140.
(32) Stoll, S.; Schweiger, A. EasySpin, a Comprehensive Software Package for Spectral Simulation and Analysis in EPR. *J. Magn. Reson.* **2006**, *178*, 42−55.
(33) Poluektov, O. G.; Filippone, S.; Martín, N.; Sperlich, A.; Deibel, C.; Dyakonov, V. Spin Signatures of Photogenerated Radical Anions in Polymer-[70]Fullerene Bulk Heterojunctions: High Frequency Pulsed EPR Spectroscopy. *J. Phys. Chem. B* **2010**, *114*, 14426−14429.
(34) Niklas, J.; Mardis, K. L.; Banks, B. P.; Grooms, G. M.; Sperlich, A.; Dyakonov, V.; Beaupré, S.; Leclerc, M.; Xu, T.; Yue, L.; et al. Highly-Efficient Charge Separation and Polaron Delocalization in Polymer−Fullerene Bulk-Heterojunctions: A Comparative Multi-Frequency EPR and DFT Study. *Phys. Chem. Chem. Phys.* **2013**, *15*, 9562−9574.
(35) Krzystek, J.; Sienkiewicz, A.; Pardi, L.; Brunel, L. C. DPPH as a Standard for High-Field EPR. *J. Magn. Reson.* **1997**, *125*, 207−211.
(36) Neese, F. The Orca Program System. *WIREs Comput. Mol. Sci.* **2012**, *2*, 73−78.
(37) Lu, T.; Chen, F. Multiwfn: A Multifunctional Wavefunction Analyzer. *J. Comput. Chem.* **2012**, *33*, 580−592.
(38) Mekenyan, O. G.; Ankley, G. T.; Veith, G. D.; Call, D. J. QSAR Estimates of Excited States and Photoinduced Acute Toxicity of Polycyclic Aromatic Hydrocarbons. *SAR QSAR Environ. Res.* **1994**, *2*, 237−247.
(39) Hare, J. P.; Kroto, H. W.; Taylor, R. Preparation and UV/Visible Spectra of Fullerenes C60 and C70. *Chem. Phys. Lett.* **1991**, *177*, 394−398.
(40) Huang, J. H.; Lee, C. P.; Ho, Z. Y.; Kekuda, D.; Chu, C. W.; Ho, K. C. Enhanced Spectral Response in Polymer Bulk Heterojunction Solar Cells by Using Active Materials with Complementary Spectra. *Sol. Energy Mater. Sol. Cells* **2010**, *94*, 22−28.
(41) Harigaya, K.; Abe, S. Optical-Absorption Spectra in Fullerenes C_{60} and C_{70}: Effects of Coulomb Interactions, Lattice Fluctuations, and Anisotropy. *Phys. Rev. B* **1994**, *49*, 16746−16752.
(42) Niu, J. Z.; Cheng, G.; Li, Z. H.; Wang, H. Z.; Lou, S. Y.; Du, Z. L.; Li, L. S. Poly(3-Dodecylthiophene) Langmuir-Blodgett Films: Preparation and Characterization. *Colloids Surf., A* **2008**, *330*, 62−66.
(43) Nijegorodov, N.; Ramachandran, V.; Winkoun, D. P. The Dependence of the Absorption and Fluorescence Parameters, the Intersystem Crossing and Internal Conversion Rate Constants on the Number of Rings in Polyacene Molecules. *Spectrochim. Acta, Part A* **1997**, *53*, 1813.
(44) Lavalette, D.; Werkhoven, C. J.; Bebelaar, D.; Langelaar, J.; Van Voorst, J. D. W. Excited Singlet State Polarization and Absorption Spectra of 1,2-Benzcoronene, 1,12-Benzperylene and 1,2:3,4-Dibenzanthracene. *Chem. Phys. Lett.* **1971**, *9*, 230−233.
(45) Joblin, C.; Salama, F.; Allamandola, L. Absorption and Emission Spectroscopy of Perylene ($C_{20}H_{12}$) Isolated in Ne, Ar, and N_2 Matrices. *J. Chem. Phys.* **1999**, *110*, 7287−7297.
(46) Niklas, J.; Poluektov, O. G. Charge Transfer Processes in OPV Materials as Revealed by EPR Spectroscopy. *Adv. Energy Mater.* **2017**, *7*, 1602226.
(47) Aguirre, A.; Gast, P.; Orlinskii, S.; Akimoto, I.; Groenen, E. J. J.; El Mkami, H.; Goovaerts, E.; Van Doorslaer, S. Multifrequency EPR Analysis of the Positive Polaron in I_2-Doped Poly(3-Hexylthiophene) and in Poly[2-Methoxy-5-(3,7-Dimethyloctyloxy)]-1,4-Phenylenevinylene. *Phys. Chem. Chem. Phys.* **2008**, *10*, 7129−7138.
(48) Konkin, A.; Ritter, U.; Scharff, P.; Roth, H.-K.; Aganov, A.; Sariciftci, N. S.; Egbe, D. A. M. Photo-Induced Charge Separation Process in (PCBM-$C_{120}O$)/(M3EH-PPV) Blend Solid Film Studied by Means of X- and K-Bands ESR at 77 and 120 K. *Synth. Met.* **2010**, *160*, 485−489.
(49) Van Landeghem, M.; Maes, W.; Goovaerts, E.; Van Doorslaer, S. Disentangling Overlapping High-Field EPR Spectra of Organic Radicals: Identification of Light-Induced Polarons in the Record Fullerene-Free Solar Cell Blend PBDB-T:ITIC. *J. Magn. Reson.* **2018**, *288*, 1−10.
(50) Sensfuss, S.; Konkin, A.; Roth, H. K.; Al-Ibrahim, M.; Zhokhavets, U.; Gobsch, G.; Krinichnyi, V. I.; Nazmutdinova, G. A.; Klemm, E. Optical and ESR Studies on Poly(3-Alkylthiophene)/Fullerene Composites for Solar Cells. *Synth. Met.* **2003**, *137*, 1433−1434.
(51) Krinichnyi, V. I.; Yudanova, E. I.; Spitsina, N. G. Light-Induced EPR Study of Poly(3-Alkylthiophene)/Fullerene Composites. *J. Phys. Chem. C* **2010**, *114*, 16756−16766.
(52) Krinichnyi, V. I.; Balakai, A. A. Light-Induced Spin Localization in Poly(3-Dodecylthiophen)/PCBM Composite. *Appl. Magn. Reson.* **2010**, *39*, 319−328.
(53) Krinichnyi, V. I.; Yudanova, E. I. Magnetic-Field-Controlled Charge Transport in Organic Polymer Composites. *Chem. Phys. Lett.* **2021**, *778*, 138787.
(54) Mizoguchi, K. Spin Dynamics in Conducting Polymers. *Makromolek. Chem.-Macromolec. Symp.* **1990**, *37*, 53−65.
(55) Marumoto, K.; Takeuchi, N.; Ozaki, T.; Kuroda, S. ESR Studies of Photogenerated Polarons in Regioregular Poly(3-Alkylthiophene)-Fullerene Composite. *Synth. Met.* **2002**, *129*, 239−247.
(56) Neaton, J. B.; Hybertsen, M. S.; Louie, S. G. Renormalization of Molecular Electronic Levels at Metal-Molecule Interfaces. *Phys. Rev. Lett.* **2006**, *97*, 216405.
(57) Xu, Y.; Chu, Q.; Chen, D.; Fuentes, A. HOMO−LUMO Gaps and Molecular Structures of Polycyclic Aromatic Hydrocarbons in Soot Formation. *Front. Mech. Eng.* **2021**, *7*, 744001.
(58) Hanazaki, I. Vapor-Phase Electron Donor-Acceptor Complexes of Tetracyanoethylene and of Sulfur Dioxide. *J. Phys. Chem.* **1972**, *76*, 1982−1989.
(59) Blase, X.; Attaccalite, C. Charge-Transfer Excitations in Molecular Donor-Acceptor Complexes within the Many-Body Bethe-Salpeter Approach. *Appl. Phys. Lett.* **2011**, *99*, 171909.
(60) Cai, Z.; Awais, M. A.; Zhang, N.; Yu, L. Exploration of Syntheses and Functions of Higher Ladder-Type Π-Conjugated Heteroacenes. *Chem.* **2018**, *4*, 2538−2570.
(61) Dyakonov, V.; Zoriniants, G.; Scharber, M.; Brabec, C. J.; Janssen, R. A. J.; Hummelen, J. C.; Sariciftci, N. S. Photoinduced Charge Carriers in Conjugated Polymer-Fullerene Composites Studied with Light-Induced Electron-Spin Resonance. *Phys. Rev. B* **1999**, *59*, 8019−8025.
(62) Kaufman, J. H.; Colaneri, N.; Scott, J. C.; Street, G. B. Evolution of Polaron States into Bipolarons in Polypyrrole. *Phys. Rev. Lett.* **1984**, *53*, 1005−1008.
(63) Baleg, A. A.; Masikini, M.; John, S. V.; Williams, A. R.; Jahed, N.; Baker, P.; Iwuoha, E. Conducting Polymers and Composites. In *Functional Polymers*; Mazumder, M. J., Sheardown, H., Al-Ahmed, A., Eds.; Springer, Cham, 2019; pp 1−54.

https://doi.org/10.1021/acs.jpcc.1c10407
J. Phys. Chem. C 2022, 126, 4495−4507

(64) Čík, G.; Šeršeň, F.; Dlháň, L. Thermally Induced Transitions of Polarons to Bipolarons in Poly(3-Dodecylthiophene). *Synth. Met.* **2005**, *151*, 124−130.
(65) Krinichnyi, V. I.; Yudanova, E. I.; Denisov, N. N.; Konkin, A. A.; Ritter, U.; Wessling, B.; Konkin, A.; Bogatyrenko, V. R. Impact of Spin-Exchange Interaction on Charge Transfer in Dual-Polymer Photovoltaic Composites. *J. Phys. Chem. C* **2020**, *124*, 10852−10869.
(66) Poole, C. P. *Electron Spin Resonance, A Comprehensive Treatise on Experimental Techniques*; John Wiley & Sons: New York, 1983.
(67) Wertz, J. E.; Bolton, J. R. *Electron Spin Resonance: Elementary Theory and Practical Applications*; Chapman and Hall: London, 2011.
(68) Krinichnyi, V. I.; Yudanova, E. I.; Denisov, N. N. Light-Induced EPR Study of Charge Transfer in Poly(3-Hexylthiophene)/Fullerene Bulk Heterojunction. *J. Chem. Phys.* **2009**, *131*, 044515.
(69) Abragam, A. *Principles of Nuclear Magnetism*; Clarendon Press: Oxford, U.K., 1983.
(70) Carrington, F.; McLachlan, A. D. *Introduction to Magnetic Resonance with Application to Chemistry and Chemical Physics*; Harrer & Row, Publishers: New York, 1967.
(71) Nechtschein, M. Electron Spin Dynamics. In *Handbook of Conducting Polymers*; Skotheim, T. A., Elsenbaumer, R. L., Reynolds, J. R., Eds.; Marcel Dekker: New York, 1997; pp 141−163.
(72) Mizoguchi, K.; Kuroda, S. Magnetic Properties of Conducting Polymers. In *Handbook of Organic Conductive Molecules and Polymers*; Nalwa, H. S., Ed.; John Wiley & Sons: Chichester, NY, 1997; Vol. 3, pp 251−317.
(73) Devreux, F.; Genoud, F.; Nechtschein, M.; Villeret, B. On Polaron and Bipolaron Formation in Conducting Polymers. In *Electronic Properties of Conjugated Polymers*; Kuzmany, H., Mehring, M., Roth, S., Eds.; Springer-Verlag: Berlin, 1987; Vol. 76, pp 270−276.
(74) Westerling, M.; Osterbacka, R.; Stubb, H. Recombination of Long-Lived Photoexcitations in Regioregular Polyalkylthiophenes. *Phys. Rev. B* **2002**, *66*, 165220.

https://doi.org/10.1021/acs.jpcc.1c10407
J. Phys. Chem. C 2022, 126, 4495−4507